Vol 17 No 7, July 2008
1674-1056/2008/17(07)/2689-07

Chinese Physics B

© 2008 Chin. Phys. Soc.
and IOP Publishing Ltd

The low-temperature mobility of two-dimensional electron gas in AlGaN/GaN heterostructures*

Zhang Jin-Feng(张金风), Mao Wei(毛 维), Zhang Jin-Cheng(张进城), and Hao Yue(郝 跃)

Key Laboratory of Ministry of Education for Wide Band-Gap Semiconductor Materials and Devices, Microelectronics Institute, Xidian University, Xi'an 710071, *China*

(Received 20 February 2008; revised manuscript received 21 March 2008)

To reveal the internal physics of the low-temperature mobility of two-dimensional electron gas (2DEG) in AlGaN/GaN heterostructures, we present a theoretical study of the strong dependence of 2DEG mobility on Al content and thickness of AlGaN barrier layer. The theoretical results are compared with one of the highest measured of 2DEG mobility reported for AlGaN/GaN heterostructures. The 2DEG mobility is modelled as a combined effect of the scattering mechanisms including acoustic deformation-potential, piezoelectric, ionized background donor, surface donor, dislocation, alloy disorder and interface roughness scattering. The analyses of the individual scattering processes show that the dominant scattering mechanisms are the alloy disorder scattering and the interface roughness scattering at low temperatures. The variation of 2DEG mobility with the barrier layer parameters results mainly from the change of 2DEG density and distribution. It is suggested that in AlGaN/GaN samples with a high Al content or a thick AlGaN layer, the interface roughness scattering may restrict the 2DEG mobility significantly, for the AlGaN/GaN interface roughness increases due to the stress accumulation in AlGaN layer.

Keywords: two-dimensional electron gas, mobility, AlGaN/GaN heterostructures, interface roughness

PACC: 7280E, 7360L

1. Introduction

The GaN-based high electron mobility transistor (HEMT) devices have been developed rapidly over the past decade. The outstanding microwave power performance of the devices, such as a record power density of over 30 W/mm,[1] are very impressive. The baseline device structure, i.e. AlGaN/GaN heterostructure, features a quantized two-dimensional electron gas (2DEG) of high sheet density (about 10^{13} cm^{-2}) and high mobility (about 1000–2500 $cm^2/(V{\cdot}s)$ at room temperature). The 2DEG property in AlGaN/GaN heterostructure depends strongly on alloy composition and thickness of the AlGaN barrier layer, and it is an important guidance to GaN HEMT design. Such a dependence of 2DEG density has been explained quite well,[2–4] but for that of 2DEG mobility, there is little theoretical research carried out though some experimental data have been reported.[2,5–10] Miyoshi *et al*[5] presented a calculation of the measured relation of the 2DEG mobility to the Al content in AlGaN barrier layer. They suggested that the lower 2DEG mobility in higher Al content sample be due to the strain-caused poor interface quality between the AlGaN layer and the GaN layer, which is partly supported by the atomic force microscopic images of the surface morphology of the samples.[5] But the theoretical analysis focused on only the interface roughness scattering and the dislocation scattering, and the effect of the other scattering mechanisms was not discussed at all.

We present in this paper a theoretical study of the low-temperature 2DEG mobility in the AlGaN/GaN heterostructures. It focuses on the dependence of the 2DEG mobility on Al content and thickness of AlGaN barrier layer. The experimental data investigated are those reported by Smorchkova *et al*[2] for a series of unintentionally doped (UID) AlGaN/GaN heterostructures at 13 K. The data are quite complete and reflect a very good consistency of the material quality, and the 2DEG mobility is highest among those available till now. The temperature is as low as 13 K, so the effect of bulk electrons can be excluded, and the mobility can be analytically modelled as a combined

*Project supported by the Key Program of the National Natural Science Foundation of China (Grant No 60736033), and Xi'an Applied Materials Innovation Fund of China (Grant No XA-AM-200703), and the Open Fund of Key Laboratory of Wide Bandgap Semiconductors Material and Devices, Ministry of Education, China.

effect of various independent scattering mechanisms. The lattice vibration scattering mechanisms considered are the acoustic deformation-potential scattering and the piezoelectric scattering, and the polar optic phonon scattering is omitted, for it is extremely weak at 13 K. The ionized impurity scattering mechanisms considered are the ionized background donor scattering and surface donor scattering. The investigated UID AlGaN/GaN sample has a not very low background electron density (about $10^{16}\,\mathrm{cm}^{-3}$), but it is too small compared with the measured 2DEG density, and the ionized surface donor states can be still ascribed to the source of the electrons for the 2DEG according to the charge balance analysis.[11,12] The dislocation scattering is included, for the dislocation is one of the major lattice defects in III–V compound materials. Also considered are inevitably the alloy disorder scattering and the interface roughness scattering.

From the analyses of the individual scattering processes and their effects on the 2DEG mobility, the internal physics of the low-temperature 2DEG mobility for AlGaN/GaN heterostructures is revealed. And it is the first theoretic analysis, to the best of our knowledge, of the 2DEG mobility as a function of the thickness of AlGaN layer in AlGaN/GaN heterostructures.

2. Model

The 2DEG mobility is modelled as $\mu^{-1} = \sum_i \mu_i^{-1}$ by using the Matheissen rule. The scattering mechanisms considered are formulated based on the 2D degenerate statistics of 2DEG. It is assumed for simplicity that screening is determined only by electrons in the lowest subband and the exact Hartree–Fork wave function is approximated by the analytical Fang–Howard variational wave function.[13] The analytical expressions of the momentum relaxation rates for the scattering mechanisms are briefly summarized below and the relevant material parameters are listed in Table 1.

The acoustic deformation-potential scattering is expressed as[14]

$$\frac{1}{\tau_{\mathrm{DP}}} = \frac{3m^* a_{\mathrm{C}}^2 k_{\mathrm{B}} T}{16\rho v_{\mathrm{s}}^2 \hbar^3} b, \tag{1}$$

where $b = \left(\dfrac{33m^* e^2 n_{\mathrm{s2D}}}{8\hbar^2 \varepsilon_0 \varepsilon_{\mathrm{s}}}\right)^{1/3}$ is a variable parameter, m^* is the electron effective mass, a_{C} is the conduction band deformation potential, k_{B} is the Boltzmann constant, T is the temperature, ρ is the mass density, v_{s} is the longitudinal acoustic phonon speed, $\hbar$ is the reduced Planck constant, e is the basic charge, n_{s2D} is the 2DEG sheet density, ε_0 is the vacuum dielectric constant, and ε_{s} is the static dielectric constant.

The piezoelectric scattering is expressed as[15]

$$\begin{aligned}\frac{1}{\tau_{\mathrm{PE}}} &= \frac{e^2 M k_{\mathrm{B}} T m^*}{4\pi\varepsilon_0\varepsilon_{\mathrm{s}}\hbar^3 k_{\mathrm{F}}^3} \\ &\quad \times \int_0^{2k_{\mathrm{F}}} \frac{F(q) q^3}{(q + q_{\mathrm{TF}} F(q))^2 \sqrt{1 - (q/(2k_{\mathrm{F}}))^2}} \mathrm{d}q, \end{aligned} \tag{2}$$

where M is the electromechanical coupling coefficient; $k_{\mathrm{F}} = \sqrt{2\pi n_{\mathrm{s2D}}}$ is the Fermi wave vector; $q = 2k_{\mathrm{F}} \sin(\theta/2)$, $\theta \in (0, \pi)$ is the difference in wave vector between the initial state and the final state in scattering; the quantity $q_{\mathrm{TF}} = m^* e^2/(2\pi\varepsilon_0\varepsilon_{\mathrm{s}}\hbar^2)$ is the Thomas–Fermi wave vector and reflects the screening length of 2DEG; $F(q) = \eta^3$ and $G(q) = (2\eta^3 + 3\eta^2 + 3\eta)/8$ with $\eta = b/(b + q)$ are two formal factors from the Fang–Howard wavefunction. The quantity $G(q)$ is present below in expressions (3), (4) and (7).

The ionized background donor scattering is expressed as[14]

$$\begin{aligned}\frac{1}{\tau_{\mathrm{IBD}}} &= N_{\mathrm{DB}} \frac{m^*}{2\pi\hbar^3 k_{\mathrm{F}}^3} \left(\frac{e^2}{2\varepsilon_0\varepsilon_{\mathrm{s}}}\right)^2 \\ &\quad \times \int_0^{2k_{\mathrm{F}}} \frac{F(q)^2 q}{[q + q_{\mathrm{TF}} G(q)]^2 \sqrt{1 - (q/(2k_{\mathrm{F}}))^2}} \mathrm{d}q, \end{aligned} \tag{3}$$

where N_{DB} is the ionized background doping density.

The surface donor scattering is expressed as[14]

$$\begin{aligned}\frac{1}{\tau_{\mathrm{SD}}} &= N_{\mathrm{SD}} \frac{m^*}{2\pi\hbar^3 k_{\mathrm{F}}^3} \left(\frac{e^2}{2\varepsilon_0\varepsilon_{\mathrm{s}}}\right)^2 \\ &\quad \times \int_0^{2k_{\mathrm{F}}} \frac{F(q)^2 \exp(-2qd) q^2}{[q + q_{\mathrm{TF}} G(q)]^2 \sqrt{1 - (q/(2k_{\mathrm{F}}))^2}} \mathrm{d}q, \end{aligned} \tag{4}$$

where the sheet density of ionized surface donor state N_{SD} can be assumed to be equal to n_{s2D} as aforementioned,[11,12] and it is changeable, for the profile or occupancy of the surface donor states in AlGaN/GaN heterostructures changes with surface barrier height when the Al content x or thickness d of AlGaN layer changes.

The dislocation scattering is expressed as[16]

$$\frac{1}{\tau_{\mathrm{DISL}}} = \frac{N_{\mathrm{disl}} m^* e^4 f^2}{\hbar^3 \varepsilon_0^2 \varepsilon_{\mathrm{s}}^2 c_0^2} \frac{1}{4\pi k_{\mathrm{F}}^4} \times \int_0^1 \frac{\mathrm{d}u}{[u + q_{\mathrm{TF}}/(2k_{\mathrm{F}})]^2 \sqrt{1-u^2}}, \quad (5)$$

where N_{disl} is the 2D density of threading edge dislocations, f is the occupancy of the states in the energy gap introduced by the dislocations, c_0 is the c-axis lattice constant and $u = q/(2k_{\mathrm{F}})$ is used for simplicity.

The alloy disorder scattering is expressed as[17]

$$\frac{1}{\tau_{\mathrm{ADO}}} = \frac{m^* \Omega(x) \Delta V^2 x(1-x)}{\hbar^3} \times \int_{-\infty}^{0} \psi^4(z) \mathrm{d}z, \quad (6)$$

where $\Omega(x) = (\sqrt{3}/2) c_0(x) a_0^2(x)$ is the volume of the unit cell of the wurtzite AlGaN, with $a_0(x)$ and $c_0(x)$ being the c plane and the c-axis lattice constants respectively; x is the Al content; ΔV is the alloy scattering potential; $\psi(z)$ is the modified Fang–Howard wavefunction.

The interface roughness scattering is expressed as[18]

$$\frac{1}{\tau_{\mathrm{IFR}}} = \frac{\Delta^2 L^2 e^4 m^*}{2(\varepsilon_0 \varepsilon_{\mathrm{s}})^2 \hbar^3} \left(\frac{1}{2} n_{\mathrm{s2D}}\right)^2 \times \int_0^1 \frac{u^4 \exp(-k_{\mathrm{F}}^2 L^2 u^2)}{[u + G(q) q_{\mathrm{TF}}/(2k_{\mathrm{F}})]^2 \sqrt{1-u^2}} \mathrm{d}u, \quad (7)$$

where Δ is the root-mean-square (RMS) roughness height, and L is the correlation length. Usually they are combined to show the interface roughness.

Table 1. The relevant material parameters used in the mobility calculation.

electron effective mass of GaN and AlGaN	$m^* = 0.20 m_0$, $m_x^* = (0.2 + 0.2x) m_0$[19] m_0 is the rest mass of electron
deformation potential of GaN	$a_{\mathrm{C}} = 9.10$ eV [20]
mass density of GaN	$\rho = 6.15$ g/cm^3[19]
longitudinal acoustic phonon speed of GaN	$v_{\mathrm{s}} = 8.00 \times 10^3$ m/s [19]
static dielectric constants of GaN and AlGaN	$\varepsilon_{\mathrm{s}} = 8.90$, $\varepsilon(x) = 8.90 - 0.40x$[19]
electromechanical coupling coefficient	$M = 0.039$[15]
lattice constant of AlGaN	$a_0(x) = (0.3189 + 0.0077x)$ nm [19] $c_0(x) = (0.5186 + 0.0204x)$ nm [19]
alloy scattering potential of AlGaN	$\Delta V = 1.80$ eV [21]
conduction band offset	$\Delta E_{\mathrm{C}}(x) = 0.75(E_{\mathrm{g}}(\mathrm{AlGaN}) – E_{\mathrm{g}}(\mathrm{GaN}))$ [2]
Thomas–Fermi wave vector	$q_{\mathrm{TF}} = 8.4994 \times 10^8 \mathrm{m}^{-1}$
dislocation filling factor	$f = 0.5$[22]

3. Comparison between theoretical and experimental results

The AlGaN/GaN structure from which the experimental data of 2DEG density and mobility are measured at $T = 13$ K is a series of UID AlGaN/GaN heterostructures grown by the molecular beam epitaxy (MBE) technique.[2] The AlGaN barrier layer is 31 nm thick for different values of Al content, and the Al mole fraction is 0.27 for different values of barrier layer thickness. It is assumed that a dislocation density (N_{disl}) is 5×10^7 cm^{-2} [10] and a background donor density (N_{DB}) is 1×10^{16} cm^{-3}.[2] The 2DEG density and mobility used in calculation are n_{sfit} and μ_{fit} fitted from the measured data n_{sexp} and μ_{exp}.

When 2DEG density varies, the 2DEG distribution changes in both the real space and the momentum space. Both 2DEG density and 2DEG distribution can affect 2DEG mobility, but the relevant analysis will be very complicated. The 2DEG distribution and its effect on 2DEG mobility can be analytically expressed by 2DEG density through the above model, so the joint effects of the 2DEG density and the 2DEG distribution on 2DEG mobility are ascribed to the effect of the 2DEG density below.

It can be deduced from the momentum relaxation rates of the considered scattering mechanisms that the acoustic deformation-potential, piezoelectric, ionized background donor and dislocation scattering are independent of barrier layer parameters. The barrier-layer-dependent scattering mechanisms include the alloy disorder scattering and the surface donor scattering. The former is related to Al content, and the latter

is related to thickness of barrier layer. The mobilities limited by all these six scattering mechanisms are calculated directly, and the overall effect of them is expressed by μ_t. A new component mobility μ_r results from $\mu_r^{-1} = \mu_{fit}^{-1} - \mu_t^{-1}$ and is ascribed to the interface roughness scattering. The interface roughness parameters are deduced from μ_r to show whether the interface roughness is dependent on alloy composition and thickness of barrier layer.

3.1. Relation between mobility and Al content

The AlGaN/GaN structures investigated are with the Al content x in barrier layer changing from 0.09 to 0.31. The 2DEG density n_{sexp} increases linearly from about 3.8×10^{12} to $1.5 \times 10^{13}\,cm^{-2}$ while the measured mobility μ_{exp} decreases almost exponentially from about 24000 to $3800\,cm^2/(V{\cdot}s)$.[2] Based on the linear fitting to the curve n_{sfit}–x, the relations between the calculated component mobilities of the individual scattering processes with the 2DEG mobility μ_{exp} and μ_{fit} are shown in Fig.1. We can see that the dominant scattering mechanisms are the alloy disorder scattering and the interface roughness scattering, and the latter is overwhelming at higher values of $x(\geq 0.25)$. The effect of the other scattering mechanisms is a little stronger at lower values of $x(\leq 0.13)$.

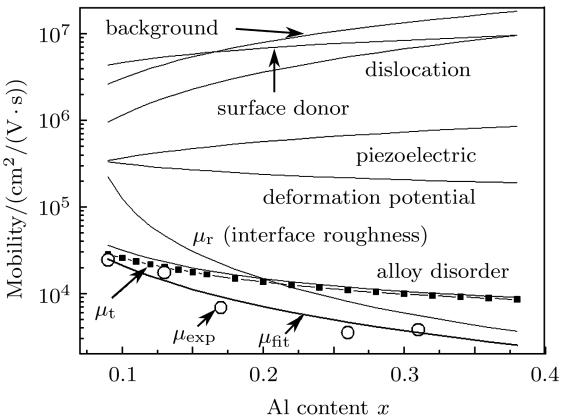


Fig.1. The experimental data of 2DEG mobility μ_{exp} at 13 K[2] with its fitting curve μ_{fit} and the calculated component mobilities of the individual scattering processes as a function of Al content x in the AlGaN barrier layer.

An Al content increase in the barrier layer results in the linear increase of 2DEG density n_{s2D} in the AlGaN/GaN heterostructures, and this is a major factor which leads to the change of various scattering processes. The dislocation scattering, the ionized background donor scattering, and the surface donor scattering are all Coulombic, and the scattering centres are the charged dislocation lines, the ionized background donor, and the surface donor states, respectively. They are weakened when n_{s2D} increases, for the screening effect of the electrons on the scattering centres is improved. The surface donor scattering mobility shows a smaller change as a result of the increased surface donor state density $N_{SD}(\approx n_{s2D})$. These scattering processes are very weak in the considered AlGaN/GaN heterostructures. This can be explained by the fact that the scattering centre density N_{disl} is too low for the dislocation scattering, and similarly N_{DB} is not high for the ionized background donor scattering. As for the surface donor scattering, the barrier layer thickness d, i.e. the Coulombic action distance between the surface donor states and the 2DEG below the barrier layer, is quite large. It should be noted that N_{disl} is generally $10^8 - 10^{11}\,cm^{-2}$ for nitride wafers, and the dislocation scattering may be an important mechanism of depressing 2DEG mobility in the AlGaN/GaN heterostructures with $x \leq 0.2$. The acoustic deformation-potential scattering mobility is proportional to $n_{s2D}^{-1/3}$, and the piezoelectric scattering mobility increases all along with n_{s2D} in the involved 2DEG density range though it has a minimum point at very low values of n_{s2D}.[13] Both of them show a T^{-1}-dependent mobility as a result of the lattice vibration, so they are quite weak at a low-temperature of 13 K.

The alloy disorder scattering in AlGaN/GaN structures originates from the effects of the randomly fluctuating Al and Ga atom potentials in the AlGaN material on the penetration part of the 2DEG wave function into the barrier layer, so it is directly related to x except for its n_{s2D} dependence. Such a scattering process is quite strong because of the large alloy scattering potential of AlGaN (1.80 eV). The alloy disorder scattering mobility is extended in $0.06 \leq x < 1$ (Fig.2) for the convenience of discussion. When n_{s2D} is higher, the 2DEG penetration is strengthened and the scattering is stronger. When x is higher, on the one hand the energy barrier at the AlGaN/GaN heterointerface is higher, which means the weaker 2DEG penetration and the weaker scattering. On the other hand, the alloy disorder extent in AlGaN (proportional to $x(1-x)$) turns stronger first and reaches its peak at $x = 0.5$, and then becomes weaker. So does the resulting alloy disorder scattering. Therefore

in the AlGaN/GaN heterostructures with x increasing while n_{s2D} being unchanged, in a range of $x \leq 0.5$ the scattering is strengthened only at small x because of the more disordered III-group atom distribution, but it is weakened when x is larger as a result of the weaker 2DEG penetration caused by the higher energy barrier at heterointerface. While in a range of $x \geq 0.5$, both the even weaker 2DEG penetration and the less disordered alloy atom distribution weaken the scattering further. As for the AlGaN/GaN heterostructures within which the 2DEG naturally changes its density with x, the alloy disorder scattering mobility reflects the interplay of the above mechanisms, and the dominant factor changes from the increase of n_{s2D} to that of x at the bottom of the mobility curve.

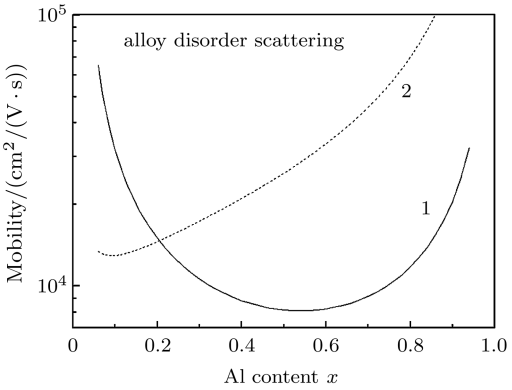


Fig.2. The alloy disorder mobility versus Al content x, where curve 1 is for calculations based on the fitted relation of $n_{s2D} - x$, and curve 2 is for calculations with a constant n_{s2D} assumed to be $10^{13}\,\mathrm{cm}^{-2}$.

The mobility μ_r shows the largest decrease in all the mobility curves in Fig.1, and it is even lower than the alloy disorder mobility when $x \geq 0.2$. This is a hint of the strong sensitivity to n_{s2D} for the interface roughness scattering. When n_{s2D} increases, the 2DEG electron distribution shifts closer to the AlGaN/GaN heterointerface and the electron transport becomes more sensitive to the structural imperfections. Meanwhile, it is expected that the pronounced change of the mobility μ_r is partially due to the AlGaN/GaN interface roughness increasing with x, which is possible because the stress in the barrier layer accumulates, and the relevant surface roughness increase has been observed.[5,6] It is necessary to know how the RMS roughness Δ and the correlation length L change with x, and this can be shown by the possible solutions of Δ and L values at given mobility and n_{s2D} (Figs.3 and 4) though we cannot extract precisely both of them from expression (7). There is an infinite series of Δ and L values theoretically which gives the same mobility values for the interface roughness scattering at a given electron density as shown in Fig.3. Though $L > 0$ is enough to solve a possible Δ, Δ_Γ at Γ point sets a lower limit for Δ. So we can set L as a constant value for μ_r to solve Δ and see how Δ changes, or to solve Δ_Γ and L_Γ. The x-dependent Δ and L are shown in Fig.4, and all of them reflect that the AlGaN/GaN interface roughness increases with increasing Al content.

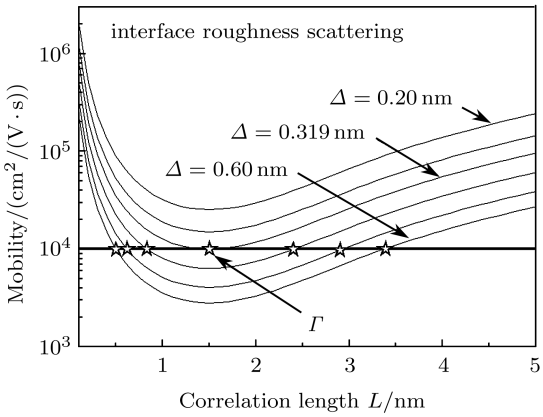


Fig.3. The interface roughness mobility at different values of RMS roughness Δ as a function of correlation length L at a 2DEG electron density of $10^{13}\,\mathrm{cm}^{-2}$. The star symbols show the possible solutions of Δ and L for a given mobility of $10^4\,\mathrm{cm}^2/(\mathrm{V{\cdot}s})$.

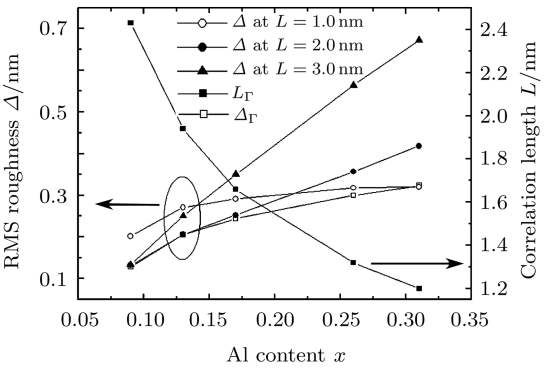


Fig.4. The calculated interface roughness parameters Δ and L for mobility μ_r in Fig.1 as a function of Al content x.

3.2. Relation between mobility and barrier layer thickness

The AlGaN/GaN structures investigated are with the barrier layer thickness d changing from 6 to 50 nm. The 2DEG density n_{sexp} increases nonlinearly from about 4.7×10^{12} to $1.4 \times 10^{13}\,\mathrm{cm}^{-2}$ while the measured mobility μ_{exp} decreases almost exponentially from about 15500 to $1500\,\mathrm{cm}^2/(\mathrm{V{\cdot}s})$. Based on the least-square fitting curve $n_{sfit} - d$ shown in Fig.5, the

relations between the calculated component mobilities of the individual scattering processes with the 2DEG mobility $\mu_{\rm exp}$ and $\mu_{\rm fit}$ are shown in Fig.6. The dominant scattering mechanisms are the alloy disorder scattering and the interface roughness scattering, and the latter is overwhelming when d is larger than 20 nm. The effect of the other scattering mechanisms, especially the surface donor scattering mechanism, is stronger when d is smaller than 10 nm.

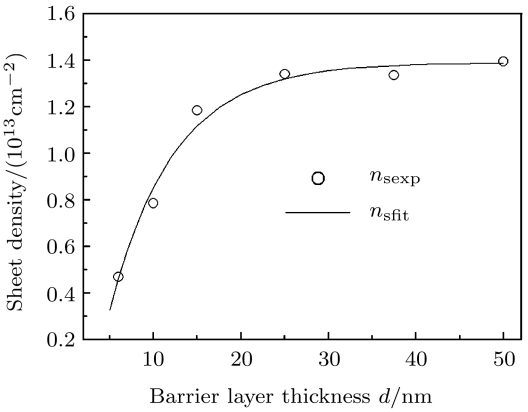


Fig.5. The 2DEG sheet density versus the barrier layer thickness d, with the experimental data $n_{\rm sexp}$[2] fitted by $n_{\rm sfit}$.

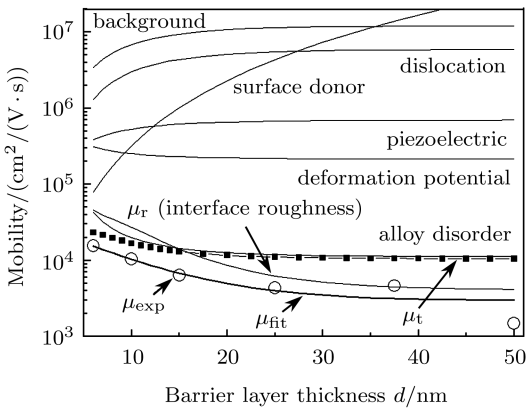


Fig.6. The experimental data of 2DEG mobility $\mu_{\rm exp}$ at 13 K[2] with its fitting curve $\mu_{\rm fit}$ and the calculated component mobilities of the individual scattering processes as a function of barrier layer thickness d.

The mobilities of dislocation, ionized background donor, deformation-potential, piezoelectric and alloy disorder scattering change with d in their own way, which reflects their dependence on $n_{\rm s2D}$ just as analysed in the last section. A common point for them is that there is a clear transition region at about $d = 20$ nm with the change in the mobility curves slowing down, which is related to the start of the saturation of 2DEG density (Fig.5). While the surface donor scattering shows a strong d dependence. When the distance between the surface donor and the 2DEG electrons is small, the Coulombic scattering is quite strong. But the scattering is weakened at higher values of d by a joint effect of the increasing $n_{\rm s2D}$ and the decreasing coulomb repulsion. So the mobility curve shows a rapid increase.

The mobility $\mu_{\rm r}$ corresponding to the interface roughness scattering decreases greatly even after the saturation point of $n_{\rm s2D}$ at about $d = 20$ nm, which is a hint of the increased AlGaN/GaN interface roughness. The possible parameter values for Δ and L are calculated in a way the same as that in the last section and shown in Fig.7. The interface roughness is found to increase with the barrier layer thickness, and it is expected to be due to the stress accumulation in the barrier layer. An exception is that the calculated value of Δ at $d = 6$ nm is generally too high and deviates from the smoothly changed Δ curve in a range of $d \geq 10$ nm. A possible explanation is that a nominal barrier layer thickness of $d = 6$ nm is lower than the real value, therefore the 2DEG mobility at $d = 6$ nm is underestimated. So the interface roughness scattering mobility at that point is also underestimated, which corresponds to too strong a scattering and too high a value of Δ.

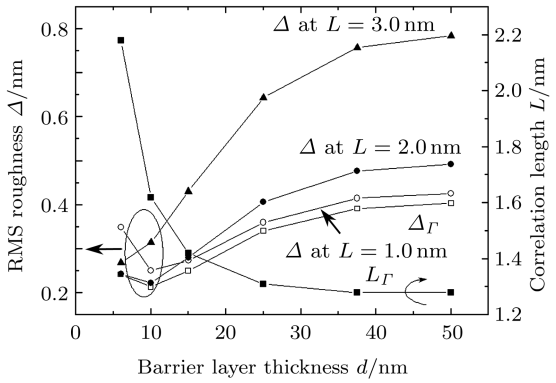


Fig.7. The calculated interface roughness parameters Δ and L for the mobility $\mu_{\rm r}$ in Fig.6 as a function of barrier layer thickness d.

4. Conclusions

This work aims to explain the dependence of low-temperature 2DEG mobility in the AlGaN/GaN heterostructures on Al content and thickness of AlGaN barrier layer. The effects of practical scattering processes are analysed, and the dominant scattering mechanisms are the alloy disorder scattering

and the interface roughness scattering at low temperature. The factors that lead to a decrease in 2DEG mobility with the barrier layer include (i) the increase of 2DEG electron density and the accompanying change of 2DEG distribution, (ii) some special scattering mechanisms directly related to the barrier layer parameters, i.e. the alloy disorder scattering dependent on Al content and the surface donor scattering dependent on the barrier layer thickness, and (iii) the AlGaN/GaN interface roughness increase at higher values of Al content or large thicknesses of the AlGaN layer as a result of stress accumulation. In all these three factors the first is the most important in the considered ranges of the barrier layer parameters. It is suggested from the calculation that the interface roughness scattering may restrict the 2DEG mobility significantly for AlGaN/GaN samples with high values Al content or thick AlGaN layers, and the relevant details need further support of the experimental investigation. It should also be noted that the effort to improve low-temperature 2DEG mobility through reducing 2DEG electron density by the AlGaN layer design may be restricted by the dislocation scattering or the surface donor scattering.

References

[1] Wu Y F, Saxler A, Moore M, Smith R P, Sheppard S, Chavarkar P M, Wisleder T, Mishra U K and Parikh P 2004 *IEEE Electron Device Lett.* **25** 117

[2] Smorchkova I P, Elsass C R, Ibbetson J P, Vetury R, Heying B, Fini P, Haus E, Denbaars S P, Speck J S and Mishra U K 1999 *J. Appl. Phys.* **86** 4520

[3] Ambacher O, Smart J, Shealy J R, Weimann N G, Chu K, Murphy M, Schaff W J, Eastman L F, Dimitrov R, Wittmer L, Stutzmann M, Rieger W and Hilsenbeck 1999 *Jpn. J. Appl. Phys.* **85** 3222

[4] Ambacher O, Foutz B, Smart J, Shealy J R, Weimann N G, Chu K, Murphy M, Sierakowski A J, Schaff W J, Eastman L F, Dimitrov R, Mitchell A and Stutzmann M 2000 *J. Appl. Phys.* **87** 334

[5] Miyoshi M, Egawa T and Ishikawa H 2005 *J. Vac. Sci. Technol.* B **23** 1527

[6] Keller S, Parish G, Fini P T, Heikman S, Chen C H, Zhang N, DenBaars S P, Mishra U K and Wu Y F 1999 *J. Appl. Phys.* **86** 5850

[7] Wu Y F, Keller B P, Fini P, Keller S, Jenkins T J, Kehias L T, Denbaars S P and Mishra U K 1998 *IEEE Electron Device Lett.* **19** 50

[8] Arulkumaran S, Egawa T, Ishikawa H and Jimbo T 2003 *J. Vac. Sci. Technol.* B **21** 888

[9] Miyoshi M, Sakai M, Ishikawa H, Egawa T, Jimbo T, Tanaka M and Oda O 2004 *J. Cryst. Growth* **272** 293

[10] Elsass C R, Poblenz C, Heying B, Fini P, Petroff P M, Denbaars S P, Mishra U K, Speck J S, Saxler A, Elhamrib S and Mitchel W C 2001 *Jpn. J. Appl. Phys.* Part 1 **40** 6235

[11] Ridley B K, Ambacher O and Eastman L F 2000 *Semicond. Sci. Technol.* **15** 270

[12] Ibbetson J P, Fini P T, Ness K D, DenBarrs S P, Speck J S and Mishra U K 2000 *Appl. Phys. Lett.* **77** 250

[13] Fang F F and Howard W E 1966 *Phys. Rev. Lett.* **16** 797

[14] Davies J H 1998 *The Physics of Low Dimensional Semiconductor* (Cambridge: Cambridge University Press)

[15] Zanato D, Gokden S, Balkan N, Ridley B K and Schaff W 2004 *Semicond. Sci. Tech.* **19** 427

[16] Jena D, Gossard A C and Mishra U K 2000 *Appl. Phys. Lett.* **76** 1707

[17] Bastard G 1983 *Appl. Phys. Lett.* **43** 591

[18] Ferry D K and Goodnick S M 1999 *Transport in Nanostructures* (Cambridge: Cambridge University Press)

[19] Levinshtein M E, Rumyantsev S L and Shur M S 2001 *Properties of Advanced Semiconductor Materials GaN, AlN, InN, BN, SiC, SiGe* (New York: John Wiley & Sons)

[20] Knap W, Contreras S, Alause H, Skierbiszewski C, Camassel J, Dyakonov M, Robert J L, Yang J, Chen Q, Khan M A, Sadowski M L, Huant S, Yang F H, Goian M, Leotin J and Shur M S 1997 *Appl. Phys. Lett.* **70** 2123

[21] Jena D 2003 *Polarization Induced Electron Populations in III-V Nitride Semiconductors: Transport, Growth, and Device Applications* (PhD thesis of University of California, Santa Barbara)

[22] Schaadt D M, Miller E J, Yu E T and Redwing J M 2001 *Appl. Phys. Lett.* **78** 88